JOURNAL OF CATALYSIS 131, 156–166 (1991)

Molybdenum Disulfide as a Hydrogen Evolution Catalyst for Water Photodecomposition on Semiconductors

ANDRZEJ SOBCZYNSKI

Institute of Chemical Technology and Engineering, Technical University, Pl. Slodowskiej-Curie 2, 60-965 Poznan, Poland

Received June 6, 1990; revised February 19, 1991

Six samples of silica-supported molybdenum disulfide were prepared by decomposition of MoS_3/SiO_2 in argon and hydrogen at 623, 673, and 723 K. The hexagonal MoS_2 structure was confirmed by XRD. ESR analysis showed the presence of Mo^{5+} in all the samples. Electrochemical studies showed that although silica-supported molybdenum disulfide did not manifest any photoresponse, it possessed good hydrogen evolution properties. These properties were confirmed in catalytic studies, in the presence of V^{2+} in 2 *M* H_2SO_4, and in photocatalytic studies in the presence of CdS/SiO_2 and TiO_2 as sensitizers and methanol as a sacrificial electron donor. Very high activity of the sample calcined in argon at 623 K is regarded to be caused by its special surface properties connected to the presence of a large quantity of Mo^{5+} ions. The reduction of the excess of molybdenum(V) ions by evolving hydrogen is taken into account in the explanation of a long induction period in photosensitized hydrogen production.

1. INTRODUCTION

It is well known that molybdenum compounds catalyze some chemical processes. They have also been used as chief constituents or minor components of many commercial catalysts. Silica- or alumina-supported MoS_2 has found an application, mainly in petrochemistry, as an active catalyst in the process of petroleum hydrodesulfurization. In this connection molybdenum disulfide has been a subject of many papers which dealt with catalytic or other physicochemical properties of supported or unsupported MoS_2. References (*1–10*) are some examples of them. It was concluded by some authors that the catalytically active sites, especially in hydrogen exchange reactions, are situated mainly on planes parallel to the *c*-axis while van der Waals planes, perpendicular to the *c*-axis, remain inactive (*8–10*). Moreover, coordinately unsaturated molybdenum ions on the surface, especially these with lower valence, are usually considered as the active sites for chemisorption and catalysis (*1–3, 5, 6*).

Depending on its composition (Mo : S ratio) molybdenum disulfide shows *n*- or *p*-semiconductor properties. Recent studies show that both valence and conduction bands of MoS_2 are formed by molybdenum *d*-orbitals (*12*). Direct or indirect bandgaps are 1.75 and 1.10 eV, respectively (*11, 13*). The small bandgap energy and high chemical durability, even in the presence of concentrated electrolytes, acids, and strong oxidants made the molybdenum sulfide a subject of extensive electrochemical and photoelectrochemical studies (*11–18*). For example, about 10% quantum efficiency has been found for *n*-MoS_2-based photocell for Cl^- oxidation. *n*-MoS_2 has also been studied as a photoanode for SO_2 oxidation in the presence of 6 *M* H_2SO_4 (*17*).

It was mentioned above that MoS_2 crystals show surface anisotropy: the basal and edge planes possess different catalytic and chemisorptive properties. Similarly, it has been found in electrochemical studies that the plane parallel to the *c*-axis provides centers for electron transfer reactions in absence of light while photoreactions occur on

0021-9517/91 $3.00

the van der Waals planes (*17*). The explanation is as follows (*17*): the non-bonding orbitals, d_{z^2}, which form a valence band, are situated toward the van der Waals surface while the orbitals which form a conduction band ($d_{x^2-y^2}$, d_{xy}, d_{xz}, p_x, and np_y) are oriented toward the surface parallel to the *c*-axis. These later participate in the dark electron transfer reactions. On the other hand the activation of the van der Waals surface needs formation of positive holes by electron excitation under irradiation.

Hydrogen evolution catalytic properties of pure and doped tungsten disulfide supported on colloidal silica were a subject of recent papers (*19, 20*). It was observed in photocatalytic and electrochemical studies that WS_2/SiO_2 alone was inactive as a light sensitive material. However, it showed high activity as a hydrogen evolution catalyst both in dark in the presence of a strong reductant (V^{2+}) and under irradiation when mixed with some sensitizers. Molybdenum and tungsten disulfides possess the same crystallographic structure and exhibit similar catalytic and electrochemical properties. Therefore, it seemed very reasonable to study the behavior of MoS_2 in the systems for hydrogen generation from water.

2. METHODS

2.1. MoS_2/SiO_2 Preparation

A 4% solution of ammonium sulfide in 4% ammonia was prepared by saturation of the aqueous solution of ammonia with gaseous H_2S (Fluka). Ammonium molybdate, 4.06 g, and then 20 g SiO_2 (Aerosil 200, Degussa) were added to 200 ml of the above solution. The suspension was mixed and kept at 343 K for 2 h, then it was acidified with hydrochloric acid to pH 2 to precipitate a black MoS_3. The precipitate was filtered and dried at 343 K. The raw product, MoS_3/SiO_2, was decomposed and calcined in argon or hydrogen at 623, 673, and 723 K. The resulting MoS_2/SiO_2 samples were denoted as 623Ar, 673Ar, 723Ar, 623H, 673H, and 723H, respectively. All the MoS_3/SiO_2 samples used as the precursors for MoS_2/SiO_2 were taken from the same batch.

3.2. CdS/SiO_2 Preparation

$Cd(NO_3)_2 \cdot 4H_2O$, 3.547 g, was dissolved in 250 ml H_2O and 25% aqueous solution of ammonia was added until the white precipitate was dissolved. SiO_2 (Aerosil 200, Degussa), 10 g, was added to the solution. The slurry was mixed and heated in a water bath to dry. Thus prepared, $Cd(OH)_2/SiO_2$ containing a little NH_4NO_3 was heated at about 473 K for 1 h in a stream of H_2S to remove the excess of ammonium nitrate and then at 673 K for 2 h.

2.3. Pt/SiO_2 Preparation

Silica-supported platinum catalyst, containing 2 wt% Pt, was prepared by impregnation of SiO_2 (Aerosil 200, Degussa) with the appropriate amount of H_2PtCl_6 followed by reduction in hydrogen at 473 K for 2 h.

2.4. Thermogravimetric Analysis

TG, DTG, and DTA curves of MoS_3/SiO_2 precursor were taken on a MOM (Hungary) derivatograph under argon at temperature range 293–1073 K.

2.5. MoS_2/SiO_2 Characterization

XRD measurements were performed on a TUR MG2 powder diffractometer using Cu$K\alpha$ radiation. BET specific surface areas were measured by nitrogen adsorption at 77 K using a dynamic method.

ESR measurements were performed for all MoS_2/SiO_2 samples and for commercial MoS_2/purum, Fluka/. About 40–80 mm^3 of the powders were placed in a 5-mm dimensional measuring quartz pipe. The measurements in X-band were performed at room temperature. Microwave frequency of the TE_{102} cavity of Radiopan spectrometer was 9.335 GHz. Modulation of 100 kHz with 1 mT or 0.68 mT was used; the amplification was 2×10^4 for microwave attenuation on the 5 dB level. The spectra were recorded more precisely near $g = 2.000$. Values of g

were calculated by comparison to a pattern signal ($g = 2.0036$).

For H_2 adsorption measurements MoS_2/SiO_2 was prepared *in situ* in an adsorption cell by decomposition of MoS_3/SiO_2 precursor at 623 K in an oxygen-free argon for 15 min (evolving sulfur was removed by heating the outlet of the cell) and subsequent calcination of resulting MoS_2/SiO_2 at 623, 673, or 723 K for 2 h. The H_2 adsorption was carried out at 573 K using 0.25 cm^3 pulses of the gas in 3-min intervals. The pulses were repeated until GC peaks were of a constant size (the reaction cell was mounted into the way of the GC carrier gas). The amount of the hydrogen adsorbed was determined from the difference between the H_2 introduced and that recorded by GC.

2.6. TiO_2 and CdS/SiO_2 Characterization

XRD and BET surface area measurements were performed in the manner described above (see 2.5). UV and visible reflection spectra were taken on a Specord M-40 spectrometer in the wavelength range 200–800 nm. MgO powder was used as a standard.

2.7. Catalytic Hydrogen Evolution from Acidic V^{2+} Solution

Vanadium(V) solution of 0.2 *M* in 2 *M* H_2SO_4 was prepared by dissolving V_2O_5 in an appropriate amount of sulfuric acid and water. The vanadium(V) was then reduced by zince amalgam. The reduction and storage of the resulting V^{2+} solution were done under argon.

Measurements of hydrogen evolution rates were performed in a 100-ml bottle-shape reaction cell equipped with an entrance–exit system for flowing argon and a septum for introducing samples using a syringe. A small, Pyrex-coated magnetic stirrer was used to maintain the catalyst in a suspension with the V^{2+} solution. The reaction cell was placed in a water bath at a constant temperature 298 ± 1 K. Argon which flowed through the cell during the reaction was purified on columns containing activated copper to remove traces of oxygen. The hydrogen evolved was analyzed with a gas chromatograph using a 2-m column filled with activated charcoal, and operated at 313 K and with argon as a carrier gas.

In a standard experiment, 60 ml H_2O and 2.2 ml 96% H_2SO_4 were poured into the reaction cell. The cell was closed and flushed with argon for about 0.5 h. Oxygen contamination in the outlet gas was examined on GC. Then 20 ml 0.2 *M* V^{2+} solution in 2 *M* H_2SO_4 were added using a syringe and the mixture was kept under flowing argon for 1–2 h. Separately, 4 mg of a catalyst (MoS_2/SiO_2 or Pt/SiO_2) were added to 16 ml H_2O, sonicated, and deaerated (argon) for about 1 h. An amount of 0.5 cm^3 of the catalyst slurry was added to the reaction cell using a syringe. The evolved hydrogen left the cell in a stream of argon (500 ml h^{-1}) and was sampled by the gas chromatograph every 15 or 30 min using a sampling valve.

2.8. Studies on Cu^{2+} and Ag^+ Reduction on Irradiated Semiconductors

The rate of metal cation reduction under irradiation was measured using ion-selective electrodes. The catalyst slurry was prepared by adding 0.1 g of the appropriate powder (MoS_2/SiO_2, CdS/SiO_2, or TiO_2) to 10 ml H_2O and sonication. A Pyrex reaction cell (100 ml volume) was equipped with an entrance–exit system for argon and two short necks to mount the electrodes, which were additionally tightened with rubber seals. Amounts of 74 ml H_2O, 25 ml CH_3OH and 1 ml of the catalyst slurry were poured into the reaction cell and the suspension was deaerated by flowing argon. After the electrode potential became stable, i.e., after 1.5–2 h, 1 ml $Cu(NO_3)_2$ or $AgNO_3$ solution (1×10^{-4}g Cu ml^{-1}, 2×10^{-4}g Ag ml^{-1}) was added and the suspension was irradiated with 180 W medium pressure Hg lamp. The disappearance of Cu^{2+} or Ag^+ was monitored in 5 min intervals. Standarization curves for Cu^{2+} and Ag^+ were taken in the pres-

ence of methanol ($H_2O : CH_3OH = 3 : 1$), SiO_2, and under Hg lamp irradiation.

2.9. *Studies of Hydrogen Photoproduction*

The reaction was carried out in the way described previously (*21, 22*). The reaction cell was similar to that described in Section 2.7. Before measurements the light-sensitive powder (CdS/SiO_2 or TiO_2-Merck, Lab. No. 808) and the hydrogen evolution catalyst (MoS_2/SiO_2) were added to the reaction cell which contained 65 ml H_2O, 25 ml CH_3OH, and, usually, 10 ml 1.0 *M* KOH. All deviations from this procedure are indicated in the paper. The suspension was flushed with argon and sonicated. The reaction cell was placed in a Pyrex water bath at a constant temperature 298 ± 1 K and irradiated with 180 medium pressure Hg lamp. Evolving hydrogen was analyzed by GC; see Section 2.7.

Incident light flux was measured by an oxalate–uranyl actinometry according to the procedure described by Hatchard and Parker (*23*). The light flux was found to be 15.6×10^{-2} μmol quanta per second.

2.10. *Electrochemical Measurements*

Current-voltage curves were taken on a Radius All-Purpose Electrochemical Instrument coupled to an *X-Y* recorder. Three electrodes were used: graphite (12 mm^2) working electrode, Pt counter electrode, and saturated calomel electrode as a reference one. The electrolyte was 0.5 *M* KCl solution. The solution included the slurry of MoS_2/SiO_2 (5 mg in 100 ml). The measurements were performed under flowing argon in dark and under Hg lamp irradiation. In some cases the potential of the graphite working electrode was kept constant for about 30 min and hydrogen contamination in the flowing argon was checked by GC.

3. RESULTS

3.1. *Characterization of MoS_2/SiO_2*

It was mentioned in the Experimental section that MoS_2/SiO_2 samples were prepared by calcination of MoS_3/SiO_2 under different conditions. The MoS_3/SiO_2 precursor was tested using thermogravimetric analysis. Two peaks were found in the DTA curve. An indistinct endothermic peak at about 583 K was accompanied by a loss of weight (TG and DTG curves) and was due to the MoS_3 decomposition and sulfur volatilization. Then a distinct exothermic peak in the range 623–733 K was caused by crystallization of amorphous molybdenum disulfide supported on silica. Taking into account the above results, and the fact that sublimation of MoS_2 occurs starting at 723 K, the calcination temperature was chosen between 623 and 723 K. Both inert (oxygen-free argon) and reducing (hydrogen) atmospheres were used during calcination. The amount of molybdenum was 1.15×10^{-3}mol/g SiO_2.

Two small and broad peaks were found at XRD spectra of all samples: at 2θ about 13.5–15° and 33–35°, characteristic of MoS_2 hexagonal structure (*25, 26*). According to the literature, they represent (002) and (100) crystallographic planes, i.e., the perpendicular (van der Waals) and parallel to the *c*-axis planes, respectively (*25*). Specific surface areas of the all six MoS_2/SiO_2 samples are near the same and amount to about 155 m^2g^{-1}. The specific surface area of silica alone is about 170 m^2g^{-1}. The very high surface area of the samples is the result of the presence of colloidal silica as a support.

ESR spectra of some samples, detected precisely in a small magnetic field range (around $g = 2.000$) are shown in Fig. 1. Three distinct lines are observed in all the spectra at $g = 1.95$, $g = 2.03$, and $g = 2.17$. The very narrow line at $g = 1.95$ is due to the presence of Mo^{5+} ($4d^1$ configuration) (*27*). The intensity of the line is the highest for $MoS_2/SiO_2$623Ar and it decreases with an increase of calcination temperature. The intensity of the line is small for hydrogen-reduced samples. The line is absent in the spectrum of a commercial MoS_2.

According to the literature, the value of g depends on the coordination number of Mo^{5+} (*27*). However, under the experimen-

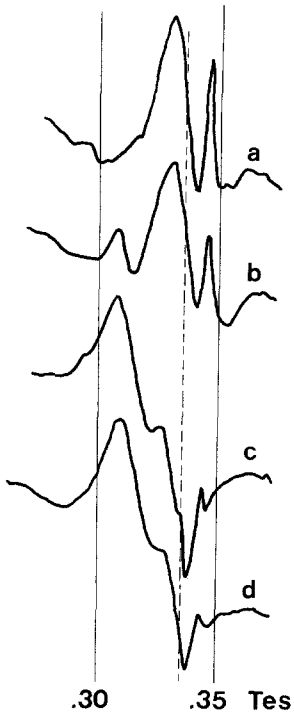

FIG. 1. ESR spectra of the samples. Dash line—g = 2.000. (a) $MoS_2/SiO_2$623Ar, (b) $MoS_2/SiO_2$723Ar, (c) $MoS_2/SiO_2$623H, (d) $MoS_2/SiO_2$723H.

tal conditions the line is not split and any conclusions cannot be drawn regarding the molybdenum(V) environment.

The other two lines, at g = 2.03 and g = 2.17, can be assigned to oxygen and sulfur radicals (*2, 28–30*). The assignment of the lines, however, is not discussed in this paper.

A small amount of hydrogen adsorption was found on the samples annealed in argon: 37.2, 18.8, and 7.1 μmol g^{-1} on the samples calcined at 623, 673, and 723 K, respectively. It can be added here that similar H_2 adsorption on MoS_2 (and WS_2) at 673 K has been described in the literature (*31*).

3.2. *Catalytic Hydrogen Evolution from Acidic V^{2+} Solution*

Catalytic properties of MoS_2/SiO_2 samples in hydrogen evolution were studied in 2 *M* H_2SO_4 solution in the presence of V^{2+}. The concentration of V^{2+} ions was chosen experimentally. It was found that in the V^{2+} concentration range 0.002–0.02 M the yield of hydrogen raised with an increase of $c_{V^{2+}}$, whereas in 0.03–0.06 *M* V^{2+} it was $c_{V^{2+}}$-independent. Therefore at $c_{V^{2+}}$ = 0.04, which was used in the studies, the catalytic reaction proceeded in a kinetic region. The amount of the catalyst was constant, i.e., 1.25×10^{-4} g.

The results of the catalytic hydrogen evolution from 0.04 *M* V^{2+} in 2 *M* H_2SO_4 on MoS_2/SiO_2 are shown in Table 1 and in Fig. 2. Additionally, for comparison reasons, Fig. 2 shows the results of H_2 evolution on Pt/SiO_2 (0.2 wt% Pt).

The activity of the all six MoS_2/SiO_2 powders is rather high: 1.25×10^{-4} g of the catalyst evolves about 0.6–2.5 ml H_2/h (about 5–21 liter h^{-1}/g MoS_2/SiO_2). The highest activity is shown by $MoS_2/SiO_2$623Ar; the activity of the other samples is 2–4 times lower. The activity depends on the calcination temperature: it lowers with a rise of calcination temperature. The activity reaches a maximum after about 30 min and then diminishes a little.

The hydrogen evolution activity of silica-supported platinum is high at the beginning of the process (see Fig. 2) and strongly decreases. It should be added here that in a blank experiment (0.2 *M* H_2SO_4, 0.04 *M* V^{2+}, 1.15×10^{-4}g SiO_2) the hydrogen was not evolved.

3.3. *Studies on Cu^{2+} and Ag^+ Reduction on Irradiated Semiconductors*

None of the MoS_2/SiO_2 samples show any photocatalytic activity when irradiated with 180 W medium pressure Hg lamp in water–methanol solutions of Cu^{2+} and Ag^+. On the other hand irradiated TiO_2 and CdS/SiO_2 caused fast reduction of both Cu^{2+} and Ag^+ ions. Figure 3 shows the results of Cu^{2+} reduction from the water–methanol solution on MoS_2/SiO_2 and TiO_2. Similar results were obtained for Ag^+ reduction on irradiated MoS_2/SiO_2, CdS/SiO_2, and TiO_2. The results are not shown in the paper.

The photoreduction of both Cu^{2+} and Ag^+

TABLE 1

Hydrogen Evolution Rates on Different MoS_2/SiO_2 Powders

Sample code	H_2 evolution rate, cm^3h^{-1}, STP[a]		
	From acidic V^{2+} solution[b]	From water–methanol–0.1 *M* KOH under irradiation[c]	
		With CdS/SiO_2	With TiO_2
$MoS_2/SiO_2$623Ar	20.8×10^3	15	21
$MoS_2/SiO_2$673Ar	9.6×10^3	12	18
$MoS_2/SiO_2$723Ar	4.8×10^3	13	19
$MoS_2/SiO_2$623H	11.2×10^3	7	14
$MoS_2/SiO_2$673H	18.8×10^3	6	13
$MoS_2/SiO_2$723H	6.4×10^3	7	12

[a] The values are referred to 1 g MoS_2/SiO_2.
[b] Maximum H_2 yield, after 0.5 h.
[c] H_2 yield at a steady-state reaction conditions.

on semiconductors were studied because of their differend redox potentials: $E^\circ_{Cu^{2+}/Cu} = 0.337$ V; $E^\circ_{Ag^+/Ag} = 0.799$ V. The conduction band potential of MoS_2/SiO_2 is shifted positively vs NHE (*17, 18, 32*) and the negative result in Cu^{2+} reduction (less positive E°) does not necessarily mean the absence of the photocatalytic activity. The energies of conduction bands of Cds and TiO_2 are negative vs NHE (*32*).

The photoreduction of Cu^{2+} or Ag^+ on semiconductors, especially on TiO_2, is well known and the kinetic and mechanism of the process were described (*33–35*). In this paper the process was applied as a test reaction to determine the photocatalytic activity of silica-supported molybdenum sulfide. The above results show that there is no photoactivity.

3.4. Hydrogen Photoproduction from Water-Methanol on MoS_2/SiO_2–CdS/SiO_2 and MoS_2/SiO_2 – TiO_2

Activities of MoS_2/SiO_2 samples as hydrogen evolution catalysts (electrocatalysts) in photosystems for hydrogen generation from water–methanol were studied in

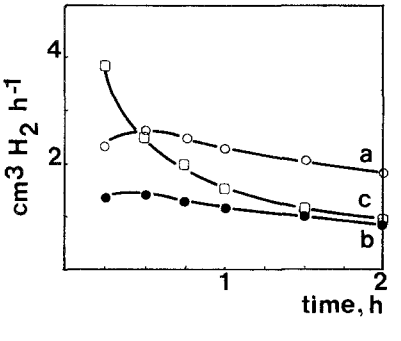

FIG. 2. Dark catalytic hydrogen evolution from acidic V^{2+} solution: (a) $MoS_2/SiO_2$623Ar, (b) $MoS_2/SiO_2$623H, (c) Pt/SiO_2.

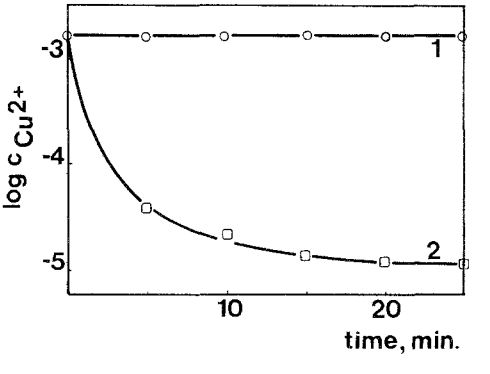

FIG. 3. Photoreduction of Cu^{2+} from water-methanol solution. Cu^{2+} concentration—1.6×10^{-5} *M*. (1) $MoS_2/SiO_2$623Ar, (2) TiO_2.

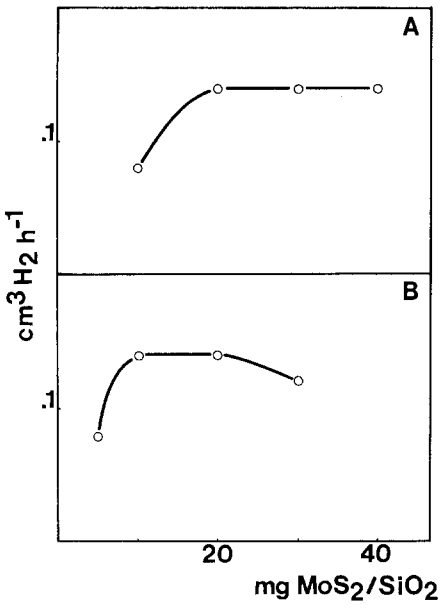

FIG. 4. Optimization of hydrogen photoproduction from water–methanol–0.1 *M* KOH on CdS/SiO_2–$MoS_2/SiO_2$623H. (A) yield of hydrogen at a constant CdS/SiO_2 : $MoS_2/SiO_2$623H ratio equal 2, (B) yield of hydrogen at a constant amount of CdS/SiO_2 equal 0.04 g.

the presence of CdS/SiO_2 and TiO_2 as photosensitizers. Both light-sensitive compounds are *n*-type semiconductors. The bandgaps are 3.0–3.2 and 2.5 eV for TiO_2 and CdS, respectively (*36, 37*). UV-visible spectra show adsorption edges at 380 nm for TiO_2 and 510 nm for CdS/SiO_2. The spectra are not shown in the paper. According to literature such adsorption edges correspond to the bandgap energies of both TiO_2 and CdS "bulk crystallites," i.e., the crystallites which do not show any effect related to their size (*38–40*).

The CdS/SiO_2 sample, prepared by sulfidation of $Cd(NO_3)_2$-impregnated silica contains 1.15×10^{-3} mol CdS/g SiO_2 (about 14 wt%). The specific surface area of the sample is 140 m^2g^{-1}. An XRD spectrum shows hexagonal CdS on amorphous SiO_2. The broadening of the XRD lines indicates very small CdS crystallites (200 Å as calculated from a Scherrer formula).

The commercial TiO_2 (Merck, Lab. No. 808) is an anatase by XRD; its specific surface area is about 6 m^2g^{-1}.

Lower limit of the light wavelength entering the reaction cell (about 300 nm) was determined by the Pyrex glass absorption edge. The upper limits of the absorbed light were determined by the bandgap energies of CdS and TiO_2.

It was found in blank tests that none of the six MoS_2/SiO_2 alone (neither the commercial MoS_2) evolved hydrogen from water–methanol in the pH range 1–13 when irradiated with 180 W medium pressure Hg lamp. Also no H_2 was found when Cd/SiO_2 and TiO_2 were illuminated in the absence of a hydrogen evolution catalyst.

Optimization of the conditions for hydrogen photoproduction from water–methanol (3 : 1) was performed using the system CdS/SiO_2–$MoS_2/SiO_2$623H. The optimum KOH concentration was 0.1 *M*: the H_2 yield lowered at higher KOH concentration, no hydrogen was found below 0.1 *M* KOH. The influence of the amount of the powders and of their weight ratio is shown in Figs. 4A and 4B. An amount of 0.04 g CdS/SiO_2 and 0.02 g MoS_2/SiO_2 was chosen as an optimum for further studies.

The results of the rate of hydrogen photogeneration from water–methanol–0.1 *M* KOH using different MoS_2/SiO_2 samples are

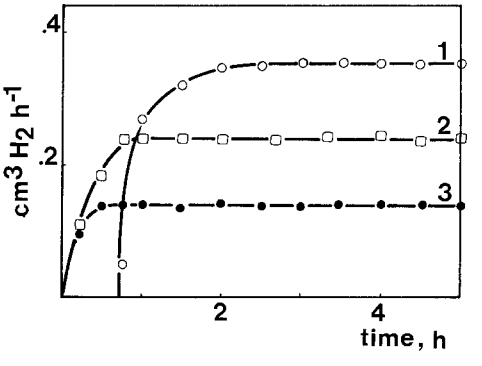

FIG. 5. Hydrogen evolution from water–methanol–0.1 *M* KOH on 0.04 g CdS/SiO_2–0.02 g MoS_2/SiO_2 with different MoS_2/SiO_2 powders. (1) MoS_2/$SiO_2$623Ar, (2) $MoS_2/SiO_2$723Ar, (3) $MoS_2/SiO_2$623H.

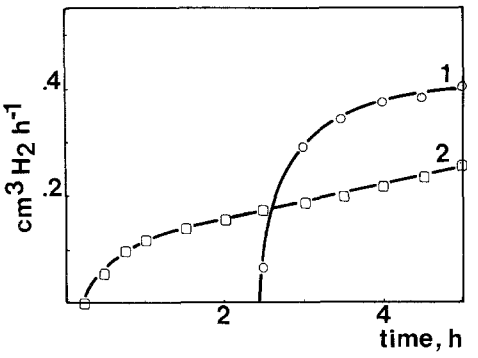

FIG. 6. Hydrogen evolution from water–methanol–0.1 *M* KOH on 0.10 g CdS/SiO_2–0.05 g MoS_2/SiO_2 with different MoS_2/SiO_2 powders. (1) $MoS_2/SiO_2$623Ar, (2) other samples.

shown in Table 1 and in Fig. 5. Figure 6 shows the hydrogen yield at a higher amount of the CdS/SiO_2–MoS_2/SiO_2 mixture. It results from the data of Table 1 and Figs. 5 and 6 that:

1. $MoS_2/SiO_2$623Ar is the most active for hydrogen photoproduction in the presence of CdS/SiO_2 as a light sensitizer (the sample was also the most active in acidic V^{2+} solution). The activity of the other two samples annealed in argon was smaller but a little higher than that of the hydrogen reduced samples.

2. Using higher amount of the CdS/SiO_2–MoS_2/SiO_2 (2 : 1) mixture the H_2 production activities were near identical for five MoS_2/SiO_2 samples; the activity of $MoS_2/SiO_2$623Ar was about 1.5 times higher.

3. Long induction period was found for the CdS/SiO_2–$MoS_2/SiO_2$623Ar system, especially at a higher amount of the powders. For other MoS_2/SiO_2 samples the induction times were relatively short.

4. After the induction period the hydrogen production rates did not alter during 5–6 h of irradiation.

The $MoS_2/SiO_2$623Ar–CdS/SiO_2 system produced about 0.3 ml H_2 per hour. If we take into account the weight of the powders and the fact that silica-supported cadmium sulfide contains 14 wt% CdS, 1 μmol CdS produces 1.7 μmol H_2 during 5 h of irradiation. Assuming that the light flux was 15.6×10^{-2} μmol quanta per second, the quantum efficiency for hydrogen photoproduction from water–methanol–0.1 *M* KOH on CdS/SiO_2–$MoS_2/SiO_2$623Ar was 4.8%. The value of the quantum efficiency was not corrected for light scattering by the catalysts particles.

Column 4 of Table 1 shows results of hydrogen generation from water–methanol–0.1 *M* KOH on irradiated MoS_2/SiO_2–TiO_2 (0.02 g MoS_2/SiO_2; 0.04 g TiO_2). As before, the highest activity was found when $MoS_2/SiO_2$623Ar was used as a hydrogen evolution catalyst. The samples annealed in argon were slightly more active than those reduced in hydrogen. The time dependence of the reaction rate was similar to that shown on Fig. 5 for MoS_2/SiO_2–CdS/SiO_2. Relatively long induction period was found when $MoS_2/SiO_2$623Ar was employed.

3.5. Electrochemical Measurements

The three-electrode system was used for measuring the catalytic hydrogen evolution properties of MoS_2/SiO_2 slurry. Figure 7 shows changes of current vs applied voltage for graphite electrode immersed in a slurry of $MoS_2/SiO_2$723H in 0.5 *M* KCl and, for

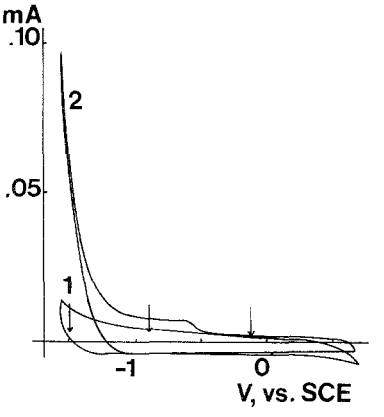

FIG. 7. Dark current vs applied voltage for graphite electrode in (1) 0.5 *M* KCl and (2) $MoS_2/SiO_2$623Ar slurry in 0.5 *M* KCl. The arrows show the electrode potentials at which H_2 evolution was measured; see text.

comparison reasons, for the electrode immersed in 0.5 *M* KCl alone. It is clear that, whereas the hydrogen evolution properties of the graphite electrode are rather poor, a big cathodic current appears when the electrode is immersed in the $MoS_2/SiO_2$723H slurry. Similar relationship of the current vs applied voltage was observed for the all six MoS_2/SiO_2 samples. No photoresponse was observed when the slurries were irradiated with 180 W medium pressure Hg lamp during the current–voltage measurements.

It was checked in separate experiments, using $MoS_2/SiO_2$723H slurry in 0.5 *M* KCl, that the cathodic current was indeed caused by the hydrogen evolution (H_3O^+ reduction). About 0.5 ml H_2 per hour was produced when the graphite electrode immersed in the $MoS_2/SiO_2$723H slurry was kept at -1.5V vs SCE. Only 0.04 ml H_2 per hour was evolved in the solution without the catalyst. No hydrogen evolution was found when the graphite electrode was kept at -0.12 and -0.90V vs SCE. The arrows on Fig. 7 show the electrode potentials at which the hydrogen evolution was measured.

4. DISCUSSION

Let us sum up the results of the physicochemical studies on MoS_2/SiO_2. The six prepared samples differ in their pretreatment; they were calcined at different temperatures: 623, 673, and 723 K and in two different atmospheres: in argon and in hydrogen. The sample precursor, silica-supported molybdenum trisulfide, undergoes different processes depending on the calcination atmosphere (*24*). In inert environment (argon) it is decomposed according to the reaction

$$MoS_3 \rightarrow MoS_2 + S \qquad (1)$$

while in hydrogen it reacts with the flowing gas according to

$$MoS_3 + H_2 \rightarrow MoS_2 + H_2S. \qquad (2)$$

Various treatments of MoS_3/SiO_2 result in different sample properties. All samples show a certain amount of Mo^{5+} ions by ESR. The highest amount of Mo^{5+} was found for $MoS_2/SiO_2$623Ar; it decreases with an increase of calcination temperature. The samples annealed in hydrogen show only very small molybdenum(V) content, independent on the temperature. It should be mentioned here that the *p*-type semiconducting properties of MoS_2 are closely related to the presence of molybdenum(V) ions or, in other words, to the excess sulfur atoms (*6*). Therefore, $MoS_2/SiO_2$623Ar should show the most *p*-character.

The samples heated in argon adsorb small amount of hydrogen (in order of 10^{16} molecules/m^2); the adsorption was not studied on samples reduced in hydrogen. There exists a strong correlation between the amount of adsorbed hydrogen and Mo^{5+} content: the sample calcined at 623 K (the richest in Mo^{5+}) adsorbs about five times more hydrogen than the sample calcined at 723 K.

$MoS_2/SiO_2$623Ar showed the highest dark catalytic hydrogen evolution activity from acidic V^{2+} solution. The activity was more than two times higher than that showed by the other samples. For both series of the samples, i.e., the argon and hydrogen ones, the activity decreased with a rise of calcination temperature. Taking into account similar electrochemical properties of the samples, i.e., similarity of their hydrogen evolution overpotentials, it can be concluded that the activity in hydrogen generation is influenced mainly by the presence of structural (surface) defects. The more disordered the structure (lower annealing temperature) the higher the activity. The most active sample, $MoS_2/SiO_2$623Ar, is the most rich in Mo^{5+}. However, the observed reduction of the molybdenum(V) ions at the beginning of H_2-generation excludes their influence on the activity.

The high activity of all the MoS_2/SiO_2 samples can be caused by good exposure to the environment of the planes parallel to the *c*-axis, thereby facilitating their interaction with the solution. On the other hand, the lack of any photoactivity shows that the van der Waals planes are not well devel-

oped—note that the crystalline form of all the MoS_2/SiO_2 samples is very poor.

The mechanism of catalytic hydrogen generation from the solution of a reduction agent or photosensitized hydrogen production from water on dispersed noble metal "microelectrodes" has been proposed by Miller *et al.* (*41, 42*). The mechanism includes electron transfer from the reductor or excited sensitizer molecule to the metal and subsequent H_3O^+ reduction by negatively charged microelectrodes. Similar mechanism of electron transfer from sensitizer to semiconductor microcrystals has been also described in the literature (*43*). The above two-step mechanism is adopted in the paper both for hydrogen generation from V^{2+} acidic solution on MoS_2/SiO_2 and for its photoproduction from water–methanol in the presence of CdS/SiO_2 and TiO_2 as sensitizers.

MoS_2/SiO_2 in photosystems with sensitizers like CdS/SiO_2 and TiO_2 efficiently generates hydrogen from water–methanol–0.1 *M* KOH. Similar to the V^{2+} solution, the most active is $MoS_2/SiO_2$623Ar. Differences in the activity between the other five samples, however, are much bigger than these observed in the acidic V^{2+} solution.

For mechanical mixtures of MoS_2/SiO_2 and CdS/SiO_2 or TiO_2 the interactions between the grains are of the great importance in addition to the interaction between the surface of MoS_2 and the solution. They can facilitate or retard the electron transfer processes from excited semiconductor particles to MoS_2/SiO_2 catalysts. In the previous studies (*44*) the agglomeration of $Pt/TiO_2/SiO_2$ and CdS_2/SiO_2 was found to be crucial for efficient hydrogen photoproduction from water–methanol–KOH using light sufficient to excite cadmium sulfide only. Therefore the rate determining step of the process of hydrogen photogeneration can be controlled both by the interaction of molybdenum sulfide surface with the solution and by the intergrain interactions. The other processes, i.e., the irradiation of CdS/SiO_2 and TiO_2 and the interaction of the semiconductor sensitizers with the solution, are expected to be the same in all experiments (the same amount of powders, the same light source, etc.).

The observed dependence of the hydrogen photoproduction rate upon pH of the slurry is also a result of the alterations of the catalyst-solution and catalyst-sensitizer interactions.

Regarding the long induction period of hydrogen photogeneration using $MoS_2/SiO_2$623Ar as a catalyst is can be concluded that the reduction of Mo^{5+} by hydrogen evolution is responsible for the observed behavior. Note that the sample was the richest in Mo^{5+} and adsorbed the most of all hydrogen among the samples under study. Although the H_2 evolution experiments were performed at temperature much lower than the H_2 adsorption studies (298 and 573 K, respectively), the very reactive atomic hydrogen was formed at the first step of H_3O^+ reduction. The atomic hydrogen is regarded to reduce the excess of surface Mo^{5+} and formation of surface SH^- groups is expected.

CONCLUSIONS

Silica-supported molybdenum disulfide is highly active as a catalyst for hydrogen evolution. Its activity in acidic V^{2+} solution is similar to that of dispersed platinum. It can be concluded, partially from data in the literature, that the supported molybdenum disulfide possess planes parallel to the *c*-axis that are exposed to the environment and provide active sites for dark electron transfer processes. The samples do not show any photoactivity. Therefore, it can be concluded that the van der Waals planes are not well developed. The very high activity of the sample heated in argon at 623 K is regarded to be caused by its special surface properties related to the highly defective structure rather than to the enhanced *p*-character of the sample. Adsorption of hydrogen and reduction of the excess of Mo^{5+} ions are considered for explanation of the

observed long induction period in photosensitized hydrogen production.

ACKNOWLEDGMENTS

The author thanks Dr. B. Sczaniecki from the Institute of Molecular Physics, Polish Academy of Science, Poznan, Poland, for help in interpretation of ESR spectra. This work was supported in part by the Polish Ministry of Education.

REFERENCES

1. Farragher, A. L., and Cosse, P., *in* "Proceedings, 5th International Congress on Catalysis, Palm Beach, 1972" (J. W. Hightower, Ed.), p. 1301. North-Holland, Amsterdam, 1973.
2. Valyon, J., and Hall, W. K., *J. Catal.* **84,** 216 (1983).
3. Valyon, J., Schneiden, R. J., and Hall, W. K., *J. Catal.* **85,** 277 (1984).
4. Ramanathan, K., and Weller, S. W., *J. Catal.* **95,** 249 (1985).
5. Millman, W. S., Segawa, K. J., Smrz, D., and Hall, W. K., *Polyhedron* **5,** 169 (1986).
6. Richardson, J. T., *J. Catal.* **112,** 313 (1988).
7. Derouane, E. G., Pedersen, E., Clausen, B. S., Gabelica, Z., Candia, R., and Topsoe, H., *J. Catal.* **99,** 253 (1986).
8. Chadwick, D., and Breysse, M., *J. Catal.* **71,** 226 (1981).
9. Stevens, G. C., and Edmonds, T., *J. Less-Common Met.* **54,** 321 (1977).
10. Tanaka, K., and Okuhara, T., *J. Catal.* **78,** 155 (1982).
11. Tributsch, H., Gerischer, H., and Clemen, C., *Ber. Bunsenges. Phys. Chem.* **83,** 655 (1979).
12. Kautek, W., Gerischer, H., and Tributsch, H., *J. Electrochem. Soc.* **127,** 2471 (1980).
13. Kam, K. K., and Parkinson, B. A., *J. Phys. Chem.* **86,** 463 (1982).
14. Tributsch, H., and Bennett, J. C., *J. Electroanal. Chem.* **81,** 97 (1977).
15. Kubiak, C. P., Schneemeyer, L. F., and Wrighton, M. S., *J. Am. Chem. Soc.* **102,** 6898 (1980).
16. Kautek, W., Gerischer, H., Tributsch, H., *Ber. Bunsenges. Phys. Chem.* **83,** 1000 (1979).
17. Calabrese, G. C., and Wrighton, M. S., *J. Am. Chem. Soc.* **103,** 21 (1981).
18. Simon, R. A., Ricco, A. J., Harrison, D. J., and Wrighton, M. S., *J. Phys. Chem.* **87,** 4446 (1983).
19. Sobczynski, A., Yildiz, A., Bard, A. J., Campion, A., Fox, M. A., Mallouk, T. E., Webber, S. E., and White, J. M., *J. Phys. Chem.* **92,** 2311 (1988).
20. Sobczynski, A., Bard, A. J., Campion, A., Fox, M. A., Mallouk, T. E., Webber, S. E., and White, J. M., *J. Phys. Chem.* **93,** 401 (1989).
21. Sobczynski, A., *J. Mol. Catal.* **39,** 43 (1987).
22. Sobczynski, A., Jakubowska, T., and Zielinski, S., *Monatsh. Chem.* **120,** 101 (1989).
23. S. L. Murov, Ed., "Handbook of Photochemistry." Dekker, New York, 1973.
24. Weisser, O., and Landa, L., "Sulfide Catalysts, Their Properties and Applications." Pergamon Press, 1973.
25. Miremadi, B. K., and Morrison, S. R., *J. Catal.* **112,** 418 (1988).
26. ASTM File.
27. Luis, C., and Che, M., *J. Phys. Chem.* **91,** 2875 (1987).
28. Quingsong, L., Yansheng, L., Baoan, L., and Chin, J., Microwave R.-F.Spectr. 5, 2 (1988).
29. Stiles, D. A., Tyerman, W. J. R., Strass, O. P., and Gunming, H. E., *Car J. Chem.* **44,** 2149 (1966).
30. Dudzik, Z., and Preston, K. F., *J. Colloid. Interface Sci.* **26,** 374 (1968).
31. Frazer, D., Moyes, R., and Wells, P. B., *Stud. Surf. Sci. Catal.* **7,** 1424 (1981).
32. Gerischer, H., *in* "Solar Energy Conversion, Solid State Physics Aspects" (B. O. Seraphin, Ed.), p. 115. Springer-Verlag, Berlin/New York, 1979.
33. Reiche, H., Dunn, W. W., and Bard, A. J., *J. Phys. Chem.* **83,** 2248 (1979).
34. Herrmann, J. M., Disdier, J., and Pichat, P., *J. Phys. Chem.* **90,** 6028 (1986).
35. Ohtani, B., Okugawa, Y., Nishimoto, S., and Kagiya, T., *J. Phys. Chem.* **91,** 3550 (1987).
36. Memming, R., *Electrochim. Acta* **25,** 77 (1980).
37. Fornarini, L., Nozik, A. J., and Parkinson, B. A., *J. Phys. Chem.* **88,** 3238 (1984).
38. Matsumoto, Y., Kurimoto, J., Amagasaki, Y., and Sato, E., *J. Electrochem. Soc.* **127,** 2148 (1980).
39. Henglein, A., *Ber. Bunsenges. Phys. Chem.* **86,** 241 (1982).
40. Brus. L., *Nouv. J. Chim.* **11,** 123 (1987).
41. Miller, D. S., Bard, A. J., Mc Lendon, G. J., and Ferguson, J., *J. Am. Chem. Soc.* **103,** 5336 (1981).
42. Miller, D. S., and Mc Lendon, G. J., *J. Am. Chem. Soc.* **103,** 6791 (1981).
43. Moser, J., and Graetzel, M., *J. Am. Chem. Soc.* **106,** 6557 (1984).
44. Sobczynski, A., Bard, A. J., Campion, A., Fox, M. A., Mollouk, T. E., Webber, S. E., and White, J. M., *J. Phys. Chem.* **91,** 3316 (1987).